IEEE Access
Multidisciplinary | Rapid Review | Open Access Journal

Received May 31, 2021, accepted June 15, 2021, date of publication June 24, 2021, date of current version July 2, 2021.

Digital Object Identifier 10.1109/ACCESS.2021.3092068

Meandering Pattern 433 MHz Antennas for Ingestible Capsules

MICHAEL J. CHRISTOE[1], (Graduate Student Member, IEEE), NATTHAPORN PHAOSEREE[2], JIALUO HAN[1], ARON MICHAEL[2], (Member, IEEE), SHAGHIK ATAKARAMIANS[2], (Senior Member, IEEE), AND KOUROSH KALANTAR-ZADEH[1], (Senior Member, IEEE)

[1]School of Chemical Engineering, University of New South Wales, Sydney, NSW 2052, Australia
[2]School of Electrical Engineering and Telecommunications, University of New South Wales, Sydney, NSW 2052, Australia

Corresponding author: Kourosh Kalantar-Zadeh (k.kalantar-zadeh@unsw.edu.au)

This work was supported in part by the National Health and Medical Research Council (NHMRC) Development Grant (APP1154969).

ABSTRACT A number of design challenges are associated with in-body devices, especially ingestible capsules, including selection of operation frequency and antenna design. Operation frequency, miniaturization, gain, and interference with the environment and the internal components of ingestible capsules are all challenging factors. In this work, we design and measure the performance of miniature antennas that can be included in ingestible capsules. The meandering pattern designs are implemented with a 433 MHz center frequency which is within one of the industrial, scientific and medical (ISM) bands. The antenna patterns are rolled into cylinders to reflect their configuration inside a capsule. The effects of different antenna design features, environmental dielectric changes, and the battery locations relative to the antenna traces are explored. We show that the optimized antenna can offer acceptable performance even when the center frequency shifts due to the modulation of the dielectric constant of the media and by the insertion of batteries. Both simulations and measurements provide insight into how the meandering antenna should be designed for the desired frequency that can be expanded to other ingestible and implantable systems.

INDEX TERMS Antennas, biomedical electronics, biomedical telemetry, gastroenterology, radio frequency.

I. INTRODUCTION

Ingestible capsules are becoming more prevalent as medical devices [1]–[17]. However, the reliability of their communications systems is still challenging. One of the main components of these communications units is the antenna, which should be designed specifically to operate efficiently within the allocated communications band for the device. The 433 MHz band is frequently used by medical devices and thus also common for ingestible capsules [18]. The 433 MHz band is within the radio spectrum reserved internationally for industrial, scientific and medical (ISM) usage, which is allocated for non-telecommunications applications [18].

There are challenges for designing antennas that can be incorporated into ingestible smart capsules or implantable systems operating at 433 MHz. When the capsule travels through various segments of the gastrointestinal tract, the environment around it changes. It experiences variations in the dielectric properties of the environment that can be liquid, gaseous, or made of specific tissues [4]. This means that the capsule antenna experiences significant impedance changes, which may lead to very large changes in its characteristics. Additionally, the shape and size of the capsule pose further challenges. The capsule size and shape are limited due to the need to adhere to the typical ingestible capsule dimensions (such as dimensions used by Medtronic, Olympus, IntroMedic, Jinshan Science and Technology, and CapsoVision for their capsules [19]), which limits the available space within the capsule, imposing constraints on the dimensions of the antenna and hence restricting the possibility of making it larger to obtain higher gains. Another issue for the antenna is relevant to the components that are placed inside the capsule. These include the PCB tracks, electronic components, the components of the packaging of the capsule and perhaps more importantly the batteries. The batteries especially have critical impact on the antenna characteristics as they occupy a significant amount of the volume in the capsule, can be in close proximity to the antenna, and are also metallic.

The associate editor coordinating the review of this manuscript and approving it for publication was Jenny Mahoney.

There have been several reports that address the above challenges. Many examples can be found in the literature regarding different antenna designs that operate at 433 MHz with acceptable gain, depending on the link budget of the incorporated transmitter, for ingestible capsules. These include coil and helix [20], patch [21]–[23], and meandered pattern [24]–[26] antennas. A typical example is the work by Arefin *et al.* [27] who designed an antenna that operated at 433 MHz and addressed the space and morphology challenge by implementing a meandering antenna design. The design used a meandering patten of approximately 36 mm × 21 mm dimensions which was rolled and placed into the capsule of 12 mm diameter and 25 mm length. They have obtained an impressive scattering parameter (S_{11}), which is commonly measured as the return loss, value of approximately −34 dB at near the centre frequency. However, they did not show how the centre frequency could shift with the change in pH that results in the change of the environmental ionic conductivity. Such a shift can be quite large when the capsule moves from the acidic environment of the stomach with a pH of 2-4 to the other segments of the GI tract with a more neutral pH of 6-8 [28]–[30]. In general, centre frequency shifts in capsule antennas, which are seen when the capsule moves from one segment of the gut to another, can be accounted for by increasing the bandwidth of the antenna. However, the influence of such manipulations on the gain of the antenna should also be taken into account. While for many capsule antennas the bandwidth and gain do not show direct relationships, it is important to ensure that a desirable gain and bandwidth can be obtained.

The influence of batteries on the performance of the capsule antenna was also presented in some studies such as the one by Wang *et al.* [24]. However, it seems that many of such studies, during measurements, ignored the inclusion of the actual full encapsulation of an ingestible capsule and hence extra return loss is seen in the measurements that could be associated with the direct electrochemical coupling of antenna to the environment rather than the radiation loss.

Orientation of the capsule antenna can also affect the performance which should also be taken into consideration. Rolling patch antenna structures into capsules can significantly impact their directionality which should be explored before implementation [26], [31].

Considering the above gaps, we have designed a series of antennas based on conformal meandering patterns. We will show that one of these designs operates at 433 MHz and can provide a S_{11} value lower than −18 dB across the extreme conditions of the dielectric environment that may be seen in the gut. The measurements and simulations have been conducted with and without the presence of the battery, which emulates the practical setup seen in real ingestible capsules.

II. PROPOSED ANTENNA DESIGNS

A major issue in the antenna design for wireless ingestible or implantable devices is to reduce the size of the antenna. Antenna size is largely determined by the wavelength of the desired operating frequency. The wavelength corresponds to:

$$\lambda = \frac{c_0}{f\sqrt{\varepsilon_r}} \tag{1}$$

where λ is the wavelength, c_0 is the speed of light in free space (3×10^8 m·s^{-1}), f is the frequency and ε_r is the relative permittivity of the medium. Increasing the permittivity of the medium leads to a reduction in the wavelength, effectively reducing the required size of the antenna. At 433 MHz, the free space wavelength is nearly 700 mm which is large relative to the limited area inside an ingestible capsule. Fortunately, operating inside the human body substantially reduces the effective wavelength by almost an order of magnitude due to detuning effects resulting from the dielectric properties of human tissues. While this reduced wavelength substantially increases the feasibility of fitting an antenna of this length into an ingestible capsule, it is also necessary to consider an antenna design methodology that is highly area efficient. As such, a meandered wire pattern design is chosen so that the antenna can operate at 433 MHz in a small area.

Our antenna is a loop with reflectional symmetry around a vertical plane of the cylindrical capsule within which it is wrapped. The resonant frequency depends on the length of the loop as can be seen in the Table S1 in the Supplementary material. To adjust the resonant frequency of the antenna, the loop length needs to be modified to change the overall inductance. A meandering pattern is suitable for this purpose as it uses the small available space efficiently. The capacitance is predominantly influenced by the permittivity of the environment rather than the spacing or width of the arms of the antenna. As such, the meandering sides of the loop antenna govern the total length that allow us to adjust the center frequency of the antenna to around 433 MHz. The width of the arms and the spacing between the arms at the antenna input could be used as tuning parameters for the input impedance, while the change of the center frequency of the antenna, due to such perturbations, can be compensated. Adjusting the dimensions of the arms and meandering patterns tunes the operation frequency and the antenna gain as presented in Table S1 and seen in Fig. S1-S10. The discussion regarding the 5 more suitable designs for operation in the capsule at 433 MHz are presented in the main manuscript while the rest are presented in the Supplementary material (Fig. S1-S10).

The designs are categorised by width (horizontal dimension) into two groups: 28 mm wide antennas and 25 mm wide antennas. The former is the common size found in standard size ingestible capsules whereas the latter allows for the reduction of size for future designs. The height (vertical dimension) of the antennas is chosen according to the length of the capsule. A summary of the dimensions for each antenna design is presented in Fig. 1. The trace width and spacing of the antenna patterns are fixed at 0.5 mm.

The first three patterns are 28 mm wide (Fig. 1.). The antenna traces are divided into two adjacent mirrored sections separated by 1 mm spacing. The height does not exceed

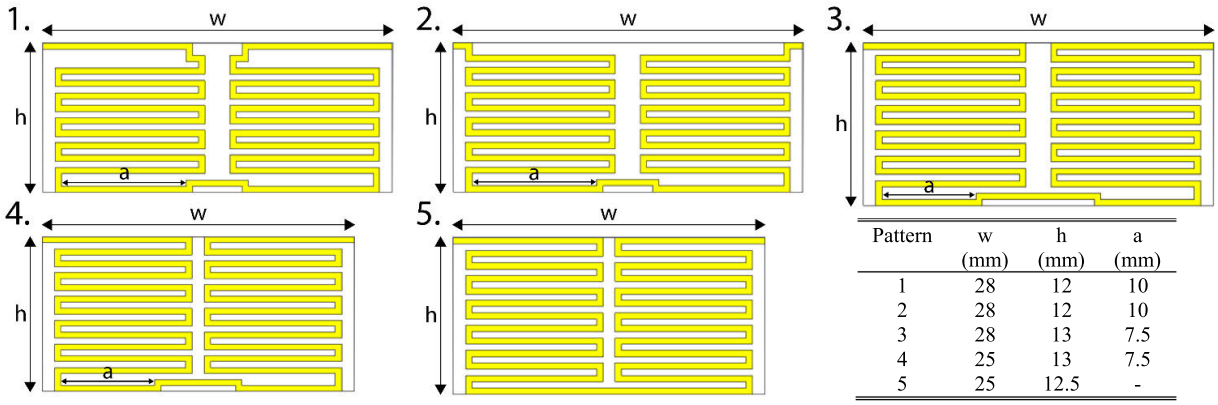

Pattern	w (mm)	h (mm)	a (mm)
1	28	12	10
2	28	12	10
3	28	13	7.5
4	25	13	7.5
5	25	12.5	-

FIGURE 1. Flat patterns of the antennas with their respective dimensions.

13 mm in all designs. The schematics of the planar form of the five antenna designs are illustrated in Fig. 1. These designs were implemented to explore the impact of introduced capacitance and inductance on the operational frequency, that are formed as a result of changing the spacing or the length of the traces [34]. For pattern 1, there is a larger space at the top of the antenna where the signal is inserted. This was introduced to see the effect of the input impedance change in comparison to other antennas. In pattern 2, the space is removed, increasing the impact of the capacitive component at the input. Another loop is added in pattern 3 to extend the total length of the antenna trace and observe the effect on gain. This slightly increases the antenna height while half of the length of the bottom spacing in pattern 3 is reduced in size to increase the internal capacitance. The last two patterns are 25 mm wide (Fig. 1). For pattern 4, the gap between the mirrored sections becomes smaller to minimize the total width of the antenna. This miniaturization also affects the total length of the antenna trace. The bottom of pattern 4 is flattened in pattern 5 to observe the effect of additional internal capacitance on the performance.

III. METHOD

A. SIMULATION SETUP

The simulations are performed in CST Studio suite (CST Microwave Studio - specialist tool for the 3D electromagnetic simulations). The antenna is modelled as a 35 μm-thick copper trace defined on a 0.1 mm-thick polyimide flexible substrate. The relative permittivity (ε_r) and loss tangent (tan δ) of polyimide are 3.5 and 0.0027, respectively [33]. The design is then rolled into a cylinder. For simulations including batteries, the antenna is wrapped around a battery analog represented by an ideal perfect electric conductor (PEC) cylinder with a height of 10.8 mm and a diameter of 7.9 mm. PEC is a good approximation of the material of the battery cladding. For comparison we also simulated the S_{11} response for a steel cladded battery, which showed no significant shift occurring to the center frequency (see supplementary

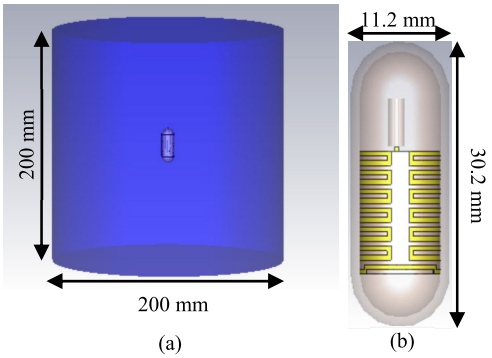

Medium	Permittivity (ε_r)	Conductivity (σ) (S/m)
Neutral water	78	1.59
Saline water	74	3.53
Ballistic gel	61.26	0.337

(c)

FIGURE 2. (a) Schematic of simulation capsule in surrounding medium. (b) Close-up schematic of simulation capsule. The capsule wall thickness is 1 mm and the substrate is on the inside of the antenna. (c) Table of dielectric properties of the three media simulated [32], [33]. The media used in simulation and measurement of the antennas in different environments were chosen to represent extreme end case conditions. As a result, the performance of the antennas across a broad range of conditions can be inferred without explicitly testing the antennas in every single variant of media found in the human body. The table representing these conditions can be found in the Supplementary material (Table S2).

material). The battery is electrically floating in the simulation and not connected to the ground of the antennas. A single end of each antenna is connected to a simulated 50 Ω coaxial cable. The coaxial cable is modelled using a two-layer cylinder shielded with a conducting material. The inner PEC cylinder is surrounded by a polytetrafluoroethylene (PTFE) insulator. Each antenna is folded inside a capsule model as shown in Fig. 2. The capsule is a polycarbonate cylinder with a dome on each end. Its relative permittivity and loss tangent

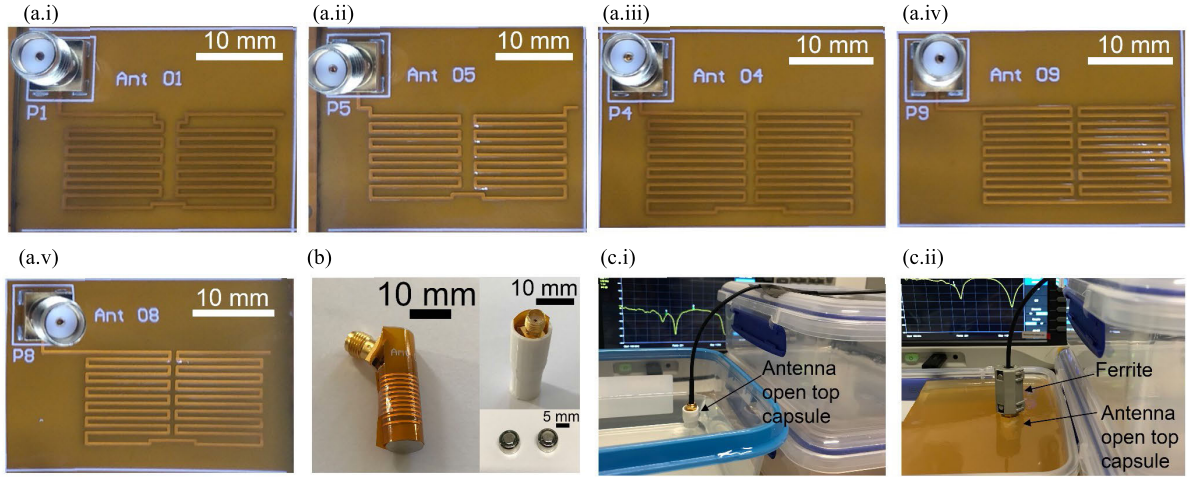

FIGURE 3. **(a) Fabricated antennas with SMA connectors (b) Antenna with batteries and the 3D printed open top test capsule (c) Measurement set-up for placing antenna with open top capsule in each medium.**

are 2.9 and 0.01, respectively [33]. As the coaxial cable needs to be placed inside the capsule to avoid the direct contact with the surrounding medium, the total capsule height and diameter of the capsules are adjusted for each design.

A simplified equivalent homogeneous human body model is simulated by a cylinder with a diameter of 200 mm and a height of 200 mm as shown in Fig. 2. The dielectric properties of the model are set to simulate three different equivalent media that are found in the gut: neutral water, saline water, and ballistic gel (that is used for describing a human tissue). Details of the dielectric properties of each medium are described in Fig. 2. The capsule is placed at the centre of the cylinder model to simulate its operation in the environment model.

B. ANTENNA FABRICATION

The planar view of the fabricated antennas can be seen in Fig. 3.a. As modelled in the simulations, 35 μm-thick meandered copper traces are fabricated on a 0.1 mm-thick polyimide flexible printed circuit board (FPCB – manufactured by PCBWay, China). One end of the copper trace is connected to a SMA connector. A complete fabricated set up that emulates the capsule and can be immersed in the measurement media is shown in Fig. 3. The antenna is rolled and placed in a capsule without top capping that was made using a 3D printer. The printed test capsule cladding is made of a 1 mm-thick layer of polylactic acid (PLA) which could perfectly protect the antenna during immersion in the liquid media, preventing it from becoming wet during the measurements. Batteries were also inserted for the battery included measurements (using two SR754 button batteries to form the battery pack). The height and the diameter of each battery pack are 5.4 mm and 7.9 mm, respectively. The battery cladding is electrically floating.

C. MEASUREMENT SETUP

To create the measurement media, 35 g of salt was dissolved in 1 L of water to replicate saline water and a mixture of 100 g of gelatine powder in 1 L of water was employed to create the ballistic gel. Tap water was used as the neutral water in the experiments. The antenna performance was evaluated using a vector network analyser (VNA – model SVA1032X) *via* a 50 Ω coaxial cable.

The measurement setup for evaluating the antenna performance is illustrated in Fig. 3.c. The antenna in the open top capsule is immersed in a plastic container filled with each test medium. The dimensions of the liquid medium container are 25 cm × 17 cm × 5 cm while that of the gel are 10 cm × 15 cm × 6 cm. A ferrite bead, with 7 mm thickness, for adjusting the impedance, was also included in some of the measurements.

Apart from testing the effect of each medium, multiple battery positions were also tested to investigate the effect of the batteries on the performance of the antenna. The batteries were placed at two different positions: at the furthest position from the antenna port and the nearest position to the antenna port. These tests were also performed without batteries. The battery position experiments were performed in each medium to measure and compare the antenna performance.

IV. RESULTS AND DISCUSSION

Fig. 4. shows the measurements with and without the ferrite in neutral and saline water (with battery inserted to account for conditions close to that of a real capsule design). The simulations are also presented for comparison. As can be seen in these graphs, the simulations are much closer in shape to the measurements taken with the ferrite. Without the ferrite, an extra trough is seen in S_{11}, which is due to the reflection of the electromagnetic waves from the coaxial cable. These extra troughs are eliminated by adding a matching ferrite. After using ferrites in the measurements, two main troughs remain in S_{11} patterns for each antenna: one is in the 400-500 MHz range and the other is in the 800-900 MHz range, which in essence are the first and second harmonics of the antenna, respectively. From this point onward we only discuss the measurements with ferrites as they represent the actual version of

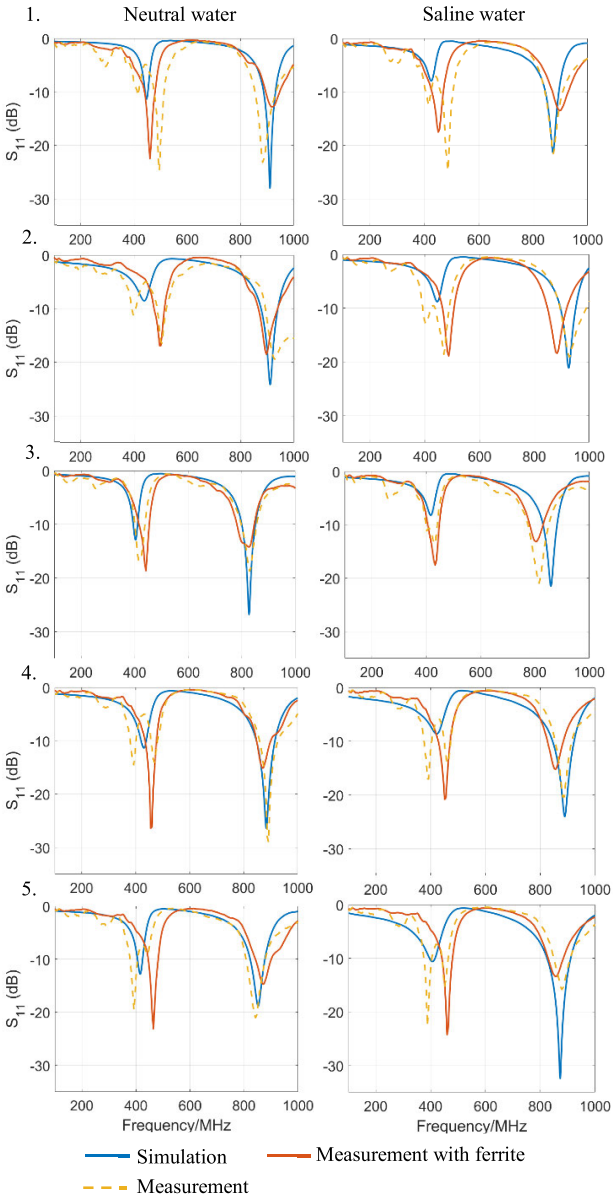

FIGURE 4. Simulations and measurements of return losses for all antenna patterns (1-5) in neutral water (left column) and saline water (right column).

the antenna responses when matching networks are implemented.

In the following, we discuss that the optimal design for the 433 MHz communications band is pattern 3. Our acceptable S_{11} was a maximum of −7dB. This was based on our past human trials and the link budget of the overall communications system. Anytime the antenna could not provide such gain we had a loss of data during the data transmission from the capsule [1]. Although the trough, for the main band, shifts from 442 MHz to 433 MHz when the medium changes from neutral water to saline water, the value of S_{11} always remains smaller than −7 dB at 433 MHz. Altogether, pattern 3 always retained a return loss of less than -7 dB at the extreme dielectric conditions as also highlighted in Table S3.

Measurements in neutral and saline water are the best indicators because they simulate the two most extreme conditions that are seen in the gut: one extreme is in the stomach with a pH of 2, which contains a high concentration of ions, and the other is when the ionic content is significantly diluted in the gut. None of the other designs offered such a consistent return loss at 433 MHz. As such, the rest of the measurements are focused on pattern 3 only.

The trends of trough shifts in the simulations are in close agreement with the measurements, although the location of the trough centre frequencies can be seen to be slightly shifted towards the lower frequencies. Altogether, the comparison of the measurements and simulations show that the simulations can be reliably used to predict the locations of troughs and the S_{11} behaviour before the actual fabrication of the proposed antennas.

Fig. 5. shows the difference in performance of pattern 3 in each of the different media tested, with and without batteries. The actual location of the battery pack relative to the antenna is shown in Fig. 6.e.ii. This location was chosen as it is the most practical location for the battery pack in an ingestible capsule. It can be seen (Fig. 5.) that the S_{11} troughs for the ballistic gel measurement conditions fall in between those of neutral and saline water, presenting an example of intermediate conditions in the gut. Additionally, it can also be seen that the centre frequencies shift to higher values when batteries are added. This is probably due to the effect of the metallic cladding of the batteries making a mirror image of the antennas where the batteries are placed.

This part cancels out the effective radiative surface of the antenna; hence the effective area of the meandering pattern is reduced and the centre frequencies are shifted to higher values.

It is important to note that while the height of the two batteries together is 10.8 mm, in practice only a few millimetres of the battery body coincide with the antenna (Fig 6.d) to impact its performance. The simulations also predict the upward shift equally well and thus agree with the measurements.

To expand the study on the full effect of the batteries at different locations relative to the antenna, further measurements were conducted (Fig. 6.). These measurements were conducted when battery locations either fully or half coincided with the antenna as shown in Fig. 6.d-e. For comparison, measurements with no battery are also included. As can be seen here (Fig. 6.a-c), when battery is fully inserted (Fig. 6.e.i) into the antenna cylinder a centre frequency shift is observed towards lower frequencies, while when the battery is only half inserted (Fig. 6.e.ii) a slight upward shift is seen. We discussed the upward shift previously. However, the significant shift downward is likely due to the impact that the metallic cladding of the battery pack has on the input impedance. It couples to the input port of the antenna and adds a very large parallel capacitance at the input of the antenna to account for this change. This accounts for a reduction of the bandwidth of the antenna as well, which is in fact undesirable as a

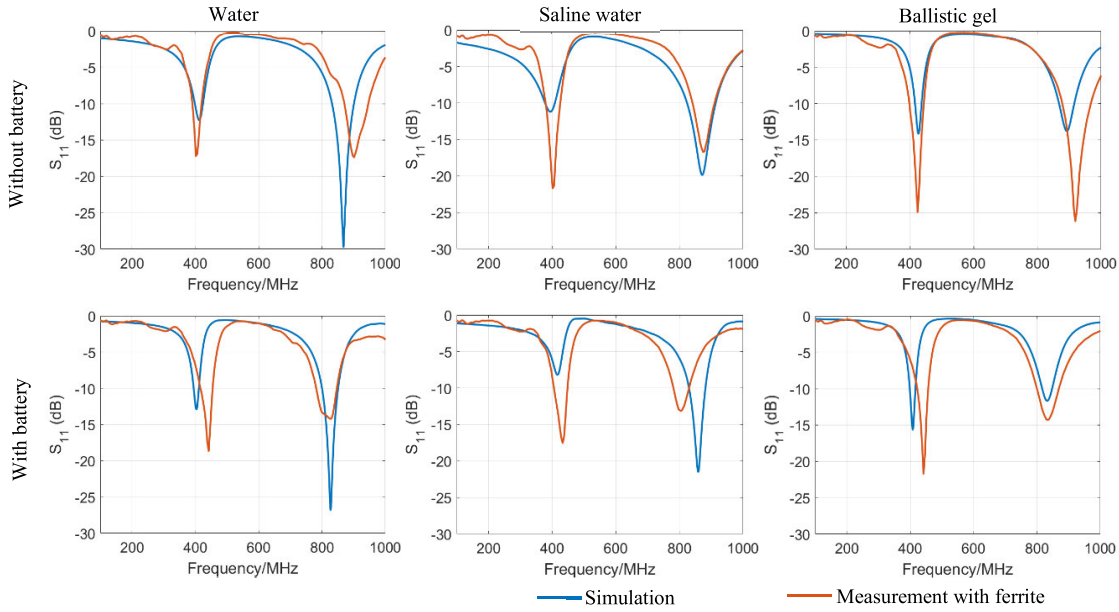

FIGURE 5. Simulations and measurements of return losses for pattern 3 in neutral water, saline water and ballistic gel, with batteries (second row) and without batteries (first row).

more broadband antenna is preferable in order to compensate for the variety of application environments. Altogether, these outcomes provide a good picture for capsule designers as to how the battery can affect the performance of the antenna.

The radiation pattern measurements were conducted in a standard set up with a cylindrical container for holding the liquid media, inside which the antenna in the protective open top capsule was partially submerged. No anechoic chamber was needed as the output power from the transmitter port of the VNA, with a minimum detection threshold for the port of -80 dB and a dynamic range of 60 dB, was -5 dBm and the probe antenna had a $\sim$25 dB loss (SRF5030T Near Field Probes E5 and H5). Considering the antenna gain of -40 to -50 dB at different orientations the system was not sensitive enough to receive signal reflections from the walls of the laboratory during the measurements (this was also confirmed in the anechoic chamber). The simulations and actual measurements of the radiation patterns for antenna pattern 3 are shown in Fig. 7. It indicates that the antenna pattern is nearly omni-directional in $\phi = 0°$ and 90° like a conventional dipole antenna. The measured peak gains of the antenna at $\varphi = 0°$ (vertical orientation) with and without battery are -41.2 dBi and -39.4 dBi, respectively, while the values for the antenna at $\varphi = 90°$ (horizontal orientation) with and without battery are -39.2 dBi and -39.0 dBi, respectively. Altogether the measured and simulated gain patterns are relatively consistent with each other. The good omnidirectionality of the designed antenna mitigates the possible loss of data during transmission, while the capsule takes various orientations inside the gut. The radiation patterns with and without the inserted battery are also relatively omni-directional.

The results show a good agreement between the simulations and the measurements in all cases. Several assumptions were made for the simulations which could influence the simulation results such as the choice of cladding material, the length of the feed line and the size of the feeding coaxial cable. The open top capsule used for measurement was designed differently than the one in the simulation as the top dome of the cladding was removed for measurements.

This might also affect the accuracy of the test environment as the position of the cable could easily change, which might lead to uncertainties in measurements.

The return loss of all the measurements fluctuated around the frequency range that covers the commercial sub-bands of MedRadio [35]. All of the designs had two troughs: one at the fundamental frequency around 400 MHz and the other at the second harmonic above 800 MHz. An additional trough could also be found near the 400 MHz band, but it was eliminated after the including of the ferrite bead. The ferrite bead was implemented as a matching network which allowed proper impedance matching between the VNA port and the antenna so that the unwanted resonance against the feeding cable could be removed.

Methods for simultaneously producing good gain and bandwidth that may involve the use of other antenna morphologies than the meandering pattern of our report are presented elsewhere [36]. However, it is important to consider that trade-offs between gain and the dimensions of antennas always remain a challenge. The small space available in capsules limits the use of a variety of designs for operation at the centre frequency of 433 MHz.

V. LIMITATIONS OF THE STUDY

The measurements could lead to more practical outcomes if we were able to test the antennas in real human bodies. However, this would require further permissions and processes including ethics approval and recruiting volunteers.

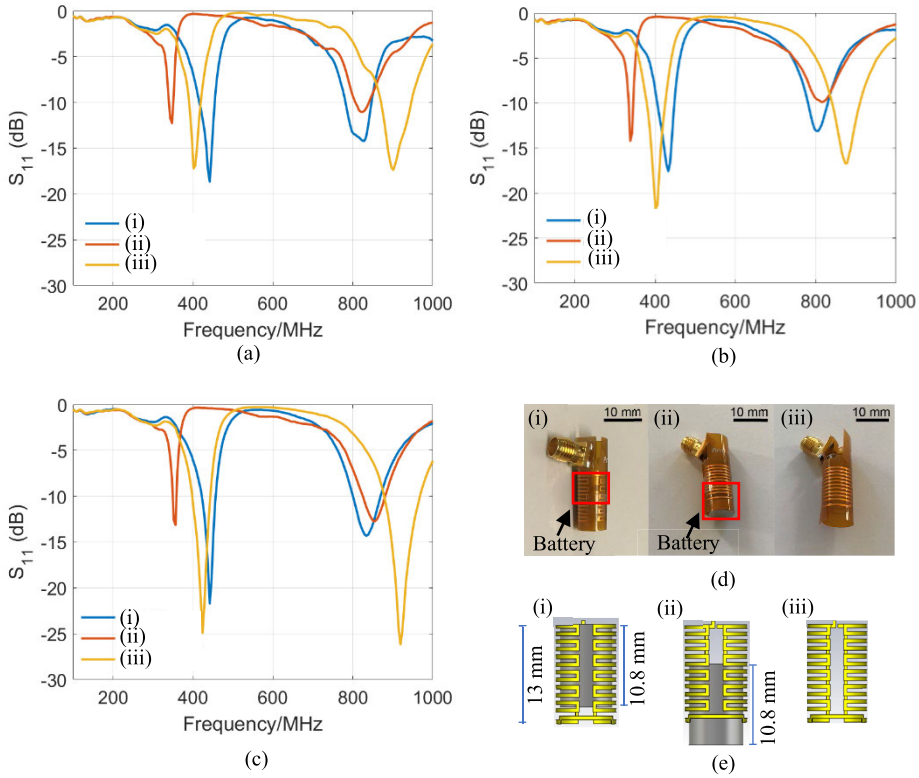

FIGURE 6. Measurements of return losses for antenna pattern 3 with different battery configurations in a) water, b) saline water, and c) ballistic gel. d) Schematics of battery configurations: i) batteries fully inserted, ii) batteries half inserted, iii) without batteries.

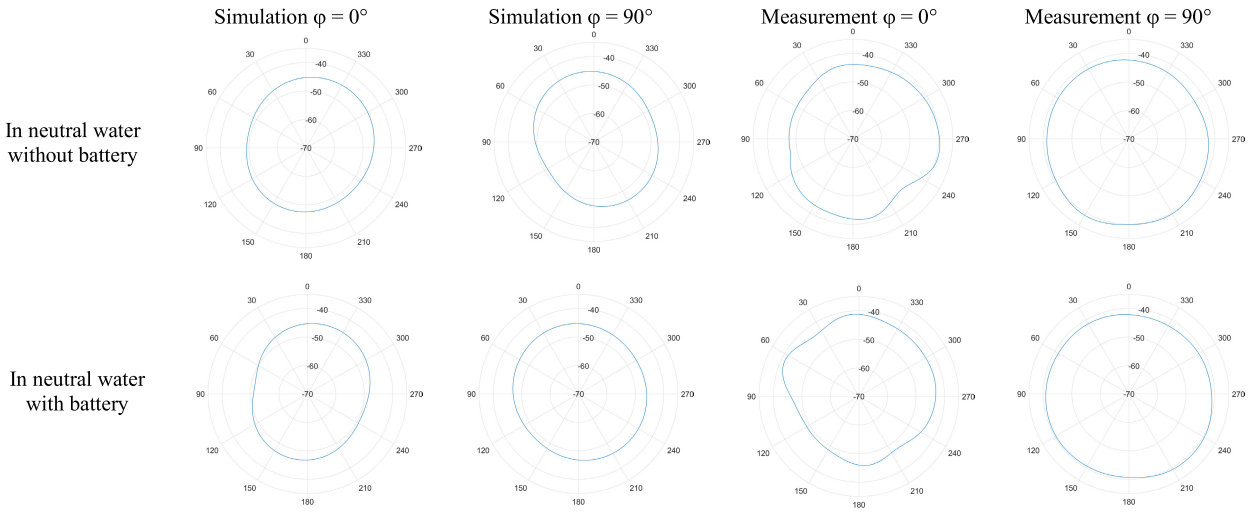

FIGURE 7. Radiation patterns for antenna pattern 3 obtained from simulation and measurement in neutral water with and without battery in two different planes.

In this paper, we have considered three different media and believe that this is sufficient to demonstrate the performance of the antennas across a broad range of dielectric conditions. Regardless, the addition of measurements in a larger variety of other dielectric environments would provide additional detail about the performance of the antennas in more specific tissue types like those found in and around specific segments of the gut.

The environment of the gut is a long tube of different diameters that contains very different gaseous, liquid or solid matter of various dielectric parameters, and the cross section of this tube changes depending on the segment of the gut. While the stomach is more like a bag, the small intestine and the colon are made of more tubular structures. An experimental setup consisting of a tube of gas, liquid or solid matter immersed in other dielectric media close to the properties of body tissues could be used for more accurately simulating the conditions present in different parts of the intestines.

Incorporating the aforementioned conditions will make the measurements of both return losses and radiation patterns

much more accurate. The same discussion can also be applied to the simulation methodology. By exploring a tubular structure of various dimensions, filled with different media (similar to ingested matter and fermented gases), inserted into a variety of dielectric substances that can represent materials ranging from different tissues to body fat, more thorough outcomes can be generated.

VI. CONCLUSION

Designing miniature antennas to maximize antenna performance is one of the most challenging tasks in the development of telecommunications subsystems for ingestible capsules. A number of meandered wire antennas were designed and tested. The designs were governed by the conditions needed to fulfill the obligations of miniaturization, performance at the required band of 433 MHz, and sufficient gain. Five meandered wire antennas were designed, simulated, fabricated, and tested in order to understand the antennas' behaviour in the environments with different dielectric properties. The return loss parameters were analysed through the simulations and measurements of the antennas immersed in neutral water, saline water, and ballistic gel with a consideration of battery positions. The simulation and measurement results showed that the antenna patterns could be modified to offer the desired performance at 433 MHz, even though it was influenced by the effect of the batteries and the change of media. The optimum antenna design could maintain a return loss of below −10 dB in every medium. The impact of multiple battery positions was also investigated for which acceptable performance was observed. Altogether, we showed that our antenna design procedure could offer sufficient wireless signal transmission strength at 433 MHz in a small device to allow for adoption in ingestible and implantable devices for future healthcare systems.

REFERENCES

[1] K. Kalantar-Zadeh, K. J. Berean, N. Ha, A. F. Chrimes, K. Xu, D. Grando, J. Z. Ou, N. Pillai, J. L. Campbell, R. Brkljača, K. M. Taylor, R. E. Burgell, C. K. Yao, S. A. Ward, C. S. McSweeney, J. G. Muir, and P. R. Gibson, "A human pilot trial of ingestible electronic capsules capable of sensing different gases in the gut," *Nature Electron.*, vol. 1, no. 1, pp. 79–87, Jan. 2018, doi: 10.1038/s41928-017-0004-x.

[2] M. Mimee, P. Nadeau, A. Hayward, S. Carim, S. Flanagan, L. Jerger, J. Collins, S. McDonnell, R. Swartwout, R. J. Citorik, V. Bulovič, R. Langer, G. Traverso, A. P. Chandrakasan, and T. K. Lu, "An ingestible bacterial-electronic system to monitor gastrointestinal health," *Science*, vol. 360, no. 6391, pp. 915–918, May 2018, doi: 10.1126/science.aas9315.

[3] C. Steiger, A. Abramson, P. Nadeau, A. P. Chandrakasan, R. Langer, and G. Traverso, "Ingestible electronics for diagnostics and therapy," *Nature Rev. Mater.*, vol. 4, no. 2, pp. 83–98, Feb. 2019, doi: 10.1038/s41578-018-0070-3.

[4] K. Kalantar-zadeh, N. Ha, J. Z. Ou, and K. J. Berean, "Ingestible sensors," *ACS Sensors*, vol. 2, no. 4, pp. 468–483, Apr. 2017, doi: 10.1021/acssensors.7b00045.

[5] A. S. Sharova, F. Melloni, G. Lanzani, C. J. Bettinger, and M. Caironi, "Edible electronics: The vision and the challenge," *Adv. Mater. Technol.*, vol. 6, no. 2, Feb. 2021, Art. no. 2000757, doi: 10.1002/admt.202000757.

[6] K. J. Berean, N. Ha, J. Z. Ou, A. F. Chrimes, D. Grando, C. K. Yao, J. G. Muir, S. A. Ward, R. E. Burgell, P. R. Gibson, and K. Kalantar-Zadeh, "The safety and sensitivity of a telemetric capsule to monitor gastrointestinal hydrogen production *in vivo* in healthy subjects: A pilot trial comparison to concurrent breath analysis," *Alimentary Pharmacol. Therapeutics*, vol. 48, no. 6, pp. 646–654, Sep. 2018, doi: 10.1111/apt.14923.

[7] K. Kalantar-zadeh, C. K. Yao, K. J. Berean, N. Ha, J. Z. Ou, S. A. Ward, N. Pillai, J. Hill, J. J. Cottrell, F. R. Dunshea, C. McSweeney, J. G. Muir, and P. R. Gibson, "Intestinal gas capsules: A proof-of-concept demonstration," *Gastroenterology*, vol. 150, no. 1, pp. 37–39, Jan. 2016, doi: 10.1053/j.gastro.2015.07.072.

[8] J. Z. Ou, C. K. Yao, A. Rotbart, J. G. Muir, P. R. Gibson, and K. Kalantar-zadeh, "Human intestinal gas measurement systems: *In vitro* fermentation and gas capsules," *Trends Biotechnol.*, vol. 33, no. 4, pp. 208–213, Apr. 2015, doi: 10.1016/j.tibtech.2015.02.002.

[9] M. Rehan, I. Al-Bahadly, D. G. Thomas, and E. Avci, "Capsule robot for gut microbiota sampling using shape memory alloy spring," *Int. J. Med. Robot. Comput. Assist. Surg.*, vol. 16, no. 5, pp. 1–14, Oct. 2020, doi: 10.1002/rcs.2140.

[10] F. N. Alsunaydih, M. S. Arefin, J.-M. Redoute, and M. R. Yuce, "A navigation and pressure monitoring system toward autonomous wireless capsule endoscopy," *IEEE Sensors J.*, vol. 20, no. 14, pp. 8098–8107, Jul. 2020, doi: 10.1109/JSEN.2020.2979513.

[11] F. N. Alsunaydih, J.-M. Redoute, and M. R. Yuce, "A locomotion control platform with dynamic electromagnetic field for active capsule endoscopy," *IEEE J. Transl. Eng. Health Med.*, vol. 6, 2018, Art. no. 1800710, doi: 10.1109/JTEHM.2018.2837895.

[12] M. S. Arefin, J.-M. Redoute, and M. R. Yuce, "Integration of low-power ASIC and MEMS sensors for monitoring gastrointestinal tract using a wireless capsule system," *IEEE J. Biomed. Health Informat.*, vol. 22, no. 1, pp. 87–97, Jan. 2018, doi: 10.1109/JBHI.2017.2690965.

[13] K. M. S. Thotahewa, J.-M. Redoute, and M. R. Yuce, "Propagation, power absorption, and temperature analysis of UWB wireless capsule endoscopy devices operating in the human body," *IEEE Trans. Microw. Theory Techn.*, vol. 63, no. 11, pp. 3823–3833, Nov. 2015, doi: 10.1109/TMTT.2015.2482492.

[14] H. Rezaei Nejad, B. C. M. Oliveira, A. Sadeqi, A. Dehkharghani, I. Kondova, J. A. M. Langermans, J. S. Guasto, S. Tzipori, G. Widmer, and S. R. Sonkusale, "Ingestible osmotic pill for *in vivo* sampling of gut microbiomes," *Adv. Intell. Syst.*, vol. 1, no. 5, Sep. 2019, Art. no. 1900053, doi: 10.1002/aisy.201900053.

[15] G. E. Banis, L. A. Beardslee, J. M. Stine, R. M. Sathyam, and R. Ghodssi, "Capacitive sensing of triglyceride film reactions: A proof-of-concept demonstration for sensing in simulated duodenal contents with gastrointestinal targeting capsule system," *Lab Chip*, vol. 20, no. 11, pp. 2020–2032, Jun. 2020, doi: 10.1039/D0LC00133C.

[16] G. E. Banis, L. A. Beardslee, J. M. Stine, R. M. Sathyam, and R. Ghodssi, "Gastrointestinal targeted sampling and sensing via embedded packaging of integrated capsule system," *J. Microelectromech. Syst.*, vol. 28, no. 2, pp. 219–225, Apr. 2019, doi: 10.1109/JMEMS.2019.2897246.

[17] Z. Bao and Y.-X. Guo, "Novel miniaturized antenna with a highly tunable complex input impedance for capsules," *IEEE Trans. Antennas Propag.*, vol. 69, no. 6, pp. 3106–3114, Jun. 2021, doi: 10.1109/TAP.2020.3037762.

[18] M. J. Christoe, J. Han, and K. Kalantar-Zadeh, "Telecommunications and data processing in flexible electronic systems," *Adv. Mater. Technol.*, vol. 5, no. 1, Jan. 2020, Art. no. 1900733, doi: 10.1002/admt.201900733.

[19] N. Hosoe, K. Takabayashi, H. Ogata, and T. Kanai, "Capsule endoscopy for small-intestinal disorders: Current status," *Digestive Endoscopy*, vol. 31, no. 5, pp. 498–507, Sep. 2019, doi: 10.1111/den.13346.

[20] J. Faerber, R. Gregson, R. E. Clutton, S. R. Khan, S. Cochran, M. P. Y. Desmulliez, G. Cummins, S. K. Pavuluri, P. Record, A. R. A. Rodriguez, H. S. Lay, R. McPhillips, B. F. Cox, and C. Connor, "*In vivo* characterization of a wireless telemetry module for a capsule endoscopy system utilizing a conformal antenna," *IEEE Trans. Biomed. Circuits Syst.*, vol. 12, no. 1, pp. 95–105, Feb. 2018, doi: 10.1109/TBCAS.2017.2759254.

[21] X. Cheng, J. Wu, R. Blank, D. E. Senior, and Y.-K. Yoon, "An omnidirectional wrappable compact patch antenna for wireless endoscope applications," *IEEE Antennas Wireless Propag. Lett.*, vol. 11, pp. 1667–1670, 2012, doi: 10.1109/LAWP.2013.2238600.

[22] M. Suzan Miah, A. N. Khan, C. Icheln, K. Haneda, and K.-I. Takizawa, "Antenna system design for improved wireless capsule endoscope links at 433 MHz," *IEEE Trans. Antennas Propag.*, vol. 67, no. 4, pp. 2687–2699, Apr. 2019, doi: 10.1109/TAP.2019.2900389.

[23] W. Lei and Y.-X. Guo, "Design of a dual-polarized wideband conformal loop antenna for capsule endoscopy systems," *IEEE Trans. Antennas Propag.*, vol. 66, no. 11, pp. 5706–5715, Nov. 2018, doi: 10.1109/TAP.2018.2862243.

[24] J. Wang, M. Leach, E. G. Lim, Z. Wang, R. Pei, and Y. Huang, "An implantable and conformal antenna for wireless capsule endoscopy," *IEEE Antennas Wireless Propag. Lett.*, vol. 17, no. 7, pp. 1153–1157, Jul. 2018, doi: 10.1109/LAWP.2018.2836392.
[25] J. Shang and Y. Yu, "An ultrawideband and conformal antenna for wireless capsule endoscopy," *Microw. Opt. Technol. Lett.*, vol. 62, no. 2, pp. 860–865, Feb. 2020, doi: 10.1002/mop.32087.
[26] A. Basir, M. Zada, Y. Cho, and H. Yoo, "A dual-circular-polarized endoscopic antenna with wideband characteristics and wireless biotelemetric link characterization," *IEEE Trans. Antennas Propag.*, vol. 68, no. 10, pp. 6953–6963, Oct. 2020, doi: 10.1109/TAP.2020.2998874.
[27] M. S. Arefin, J.-M. Redoute, and M. R. Yuce, "Meandered conformai antenna for ISM-band ingestible capsule communication systems," in *Proc. 38th Annu. Int. Conf. IEEE Eng. Med. Biol. Soc. (EMBC)*, Aug. 2016, pp. 3031–3034, doi: 10.1109/EMBC.2016.7591368.
[28] C. Gabriel, S. Gabriel, and E. Corthout, "The dielectric properties of biological tissues: I. Literature survey," *Phys. Med. Biol.*, vol. 41, no. 11, pp. 2231–2249, Nov. 1996, doi: 10.1088/0031-9155/41/11/001.
[29] S. Gabriel, R. W. Lau, and C. Gabriel, "The dielectric properties of biological tissues: II. Measurements in the frequency range 10 Hz to 20 GHz," *Phys. Med. Biol.*, vol. 41, no. 11, pp. 2251–2269, Nov. 1996, doi: 10.1088/0031-9155/41/11/002.
[30] S. Gabriel, R. W. Lau, and C. Gabriel, "The dielectric properties of biological tissues: III. Parametric models for the dielectric spectrum of tissues," *Phys. Med. Biol.*, vol. 41, no. 11, pp. 2271–2293, Nov. 1996, doi: 10.1088/0031-9155/41/11/003.
[31] M. M. Suzan, K. Haneda, C. Icheln, A. Khatun, and K.-I. Takizawa, "An ultrawideband conformal loop antenna for ingestible capsule endoscope system," in *Proc. 10th Eur. Conf. Antennas Propag. (EuCAP)*, Apr. 2016, pp. 1–5, doi: 10.1109/EuCAP.2016.7481526.
[32] E. Porter, J. Fakhoury, R. Oprisor, M. Coates, and M. Popović, "Improved tissue phantoms for experimental validation of microwave breast cancer detection," in *Proc. 4th Eur. Conf. Antennas Propag.*, Apr. 2010, pp. 1–5.
[33] *CST Studio Suite 2020*, Dassault Systèmes, Vélizy-Villacoublay, France, 2020.
[34] D. M. Pozar, *Microwave Engineering*. Hoboken, NJ, USA: Wiley, 2011.
[35] *Radio Frequency Devices (Title 47, Chapter 1, Part 15)*, US Federal Communications Comission, Washington, DC, USA, 2019.
[36] R. Alrawashdeh, "Implantable antennas for biomedical applications," Ph.D. dissertation, Dept. Elect. Eng., Liverpool Univ., Liverpool, U.K., 2015.

MICHAEL J. CHRISTOE (Graduate Student Member, IEEE) received the B.Eng. degree in electrical and electronic engineering from RMIT University, Australia, in 2018. He is currently pursuing the Ph.D. degree with the School of Chemical Engineering, University of New South Wales, Australia. His research interests include the implementation of embedded systems for small, low-power, wireless sensor applications, such as gas sensing for biomedical diagnostics, as well as using field-programmable gate arrays (FPGAs) for embedded applications requiring highly efficient computation.

NATTHAPORN PHAOSEREE received the B.S. degree in electrical engineering from Chulalongkorn University, Bangkok, Thailand, in 2012, and the M.S. degree in telecommunications from the University of New South Wales (UNSW), Sydney, Australia, in 2021. From 2013 to 2018, she was a Wireless Engineer at Huawei Technologies, Thailand, where she was involved in wireless network deployment in Thailand. She worked with the Centre for Advanced Solid and Liquid Based Electronics and Optics (CASLEO), UNSW.

JIALUO HAN received the B.E. degree from the School of Engineering, RMIT University, Australia, in 2018. He is currently pursuing the Ph.D. degree with the School of Chemical Engineering, University of New South Wales, Australia. His research interests include surface and core properties of liquid metals for enabling different applications ranging from gas sensing to MEMS.

ARON MICHAEL (Member, IEEE) received the B.E. degree (Hons.) in electrical engineering from Addis Ababa University, Addis Ababa, Ethiopia, in 1997, and the M.Eng.Sc. degree in electronics and communication and the Ph.D. degree in electrical engineering from the University of New South Wales, Sydney, Australia, in 2000 and 2007, respectively. He is currently a Lecturer with the School of Electrical Engineering and Telecommunication, University of New South Wales. He has published more than 80 scientific publications in these areas. His current research interests include microelectromechanical systems-based optical switching, optical interconnects and chip cooling, piezoelectric actuators for micro-optics, evaporated thick silicon films, and silicon photonics for ultra-high-sensitive displacement sensors.

SHAGHIK ATAKARAMIANS (Senior Member, IEEE) received the B.S. degree in telecommunication engineering from the Iran University of Science and Technology (IUST), the M.S. degree in telecommunication engineering from the University of Tehran, and the Ph.D. degree in electrical and electronic engineering from The University of Adelaide, Australia, in 2011, with a Certificate of Merit from the Dean. She is currently a Scientia Senior Lecturer and a Team Lead of the Atakaramians Laboratory, School of Electrical Engineering and Telecommunications, UNSW, Sydney. She was with the Institute of Photonics and Optical Science (IPOS), from 2011 to 2017, and also with the Centre for Ultrahigh bandwidth Devices for Optical Systems (CUDOS), from 2012 to 2014, and with the University of Sydney, first as a Postdoctoral Fellow and then as a Research Fellow. Her research interests include terahertz waveguides, metawaveguides, and meta-devices. Dr. Atakaramians is a Senior OSA Member. She was awarded the Australian Research Council (ARC) Discovery Early Career Researcher Award (DECRA), in 2014. Her Ph.D. thesis received the Gertrude Rohan Memorial Prize and the University Doctoral Research Medal for outstanding research, in 2011. She is an Associate Editor of the APL Photonics and AIP Publishing.

KOUROSH KALANTAR-ZADEH (Senior Member, IEEE) is currently a Professor of chemical engineering with the University of New South Wales (UNSW), Sydney, Australia. He has coauthored over 450 scientific articles and books. His research interests include materials sciences, electronics, and transducers. He is one of the Australian Research Council (ARC) Laureate Fellows of 2018. He is also a member of the editorial boards of journals including *American Chemical Society (ACS) Sensors*, *ACS Applied Nano Materials*, *Advanced Materials Technologies*, *Nanoscale*, and *ACS Nano*. He has received many international awards including the 2017 IEEE Sensor Council Achievement, the 2018 ACS Advances in Measurement Science Lectureship Award, and the 2020 Robert Boyle Prize for Analytical Science, Royal Society of Chemistry (RSC), U.K. His name has been present in the Clarivate Analytics most highly cited list, since 2018.